Correlation-based constellations of satellites for local telecommunication and monitoring services

M. Pontani, P. Teofilatto

Abstract

Low Earth orbit constellations deserve several advantages with respect to geostationary platforms, i.e. lower costs for satellite development and launch, increased imaging resolution, as well as reduced power requirements and signal time delays. This research is concerned with an original method for constellation design, based on the use of a correlation function. All satellites are placed in repeating ground track orbits, and two conflicting requirements are considered: the maximization of the maximum continuous coverage and the minimization of the maximum revisit time of a target area located on Earth surface. A suitable way of determining the related optimal constellation configurations is based on avoiding overlapping between visible passes of distinct satellites. With this intent, an analytic expression can be derived for the correlation function, which is employed to evaluate the overlapping between visible passes. Then an algorithmic search for the zeros of this function allows determining some constellation configurations with the desired characteristics. This heuristic method turns out to be a successful approach for constellation design and several results are reported with reference to different latitudes of the target area and distinct repeating orbits.

1. Introduction

Low Earth orbit constellations deserve several advantages with respect to geostationary platforms, i.e. lower costs for satellite development and launch, increased imaging resolution, as well as reduced power requirements and signal time delays. These circumstances have recently induced a growing interest towards low Earth orbit constellations by commercial telecommunication and navigation ventures. In general, constellation build-up strategies include, as first step, an accurate coverage analysis aimed at fixing an optimal set of parameters, such as the number of satellites and their spatial distribution, with reference to the required operational purposes. Numerical and geometrical approaches have been employed for optimizing constellation performance; this is due to the fact that analytical solutions to such optimization problems are still elusive.

Common classes of constellations include Walker symmetric rosette constellations [1-4], circular polar orbit constellations [5, 6], highly elliptical orbit constellations [7], geosynchronous orbit constellations, and polyhedral constellations [8]. Most of these constellations show a high degree of symmetry and are particularly suitable for the continuous coverage of large areas. Moreover, sparse coverage constellation design has been studied by several researchers. Constellations with a constrained (maximum) revisit time were analyzed by Der-Ming and Wen-Chiang [9] with the purpose of minimizing the number of satellites. Constellations with minimum revisit time were designed by Lang and Hanson [10]. Lang et al. [11, 12] applied a genetic algorithm in order to determine constellations such that either the maximum or the average revisit time is minimized.

This paper is concerned with an original approach to constellation design, with the final intent of optimizing the visibility properties of a target region located on the Earth surface. Two types of requirements are considered: the maximization of the maximum continuous coverage of the target, and the minimization of the maximum revisit time, which is the time interval when the target is not visible by any satellite belonging to the constellation. Clearly, these requirements are conflicting and apply to different scenarios. For instance, an adequate continuous coverage may be required for executing planned operations, whereas in other contexts (war scenarios or calamities) the capability of observing a specific location opportunely needs to be ensured. This kind of survey activity is often referred to as "early warning monitoring". Other operative situations may suggest the combination of the two mentioned basic requirements.

The method proposed in this paper is based on the use of a correlation function to perform a global search over the entire set of constellations whose satellite visible passes do not overlap. Circular orbits with repeating ground tracks are considered. These orbits were shown to have better partial coverage properties with respect to those with non repeating ground tracks [13]. In addition, the use of repeating orbits allows focusing the analysis on the period of repetition only. The visible passes over the target are translated into a binary time-dependent function, named "visibility function", which identifies the time intervals of visibility. A suitable way of increasing the continuous coverage and simultaneously reducing the revisit time consists in avoiding the overlapping among visibility functions of distinct satellites. This goal is here achieved by annihilating the correlation function, which is a direct measure of the overlapping of distinct visibility functions.

This paper is organized as follows: Section 2 defines repeating ground track orbits, whereas the method for determining the orbit elements ensuring the maximum visibility of the target area from a single satellite is described in Section 3. Section 4 is concerned with the strategy for

constellation design. The so-called "visibility function" is introduced and the correlation function is described as the central mathematical tool to derive all the time delays among satellite visible passes over the target. Section 5 presents the results (i.e. the optimal constellations) for some cases of possible interest.

2. Repeating ground track orbits

The constellation is assumed to be composed of several satellites placed in equally inclined circular orbits with an identical altitude H. In this study orbits are considered such that perturbations, as atmospheric drag, solar radiation pressure, and third body effects can be regarded as negligible for the purpose of constellation design. In contrast, Earth oblateness (J_2 zonal harmonic perturbation) produces significant effects on the orbital elements and is considered in the model. In particular, J_2 perturbation affects the right ascension of the ascending node (RAAN), Ω, the argument of perigee, ω, and the mean anomaly, M:

$$\dot{\Omega}(a,i) = -\frac{3}{2} J_2 \frac{R_E^2}{a^{\frac{7}{2}}} \sqrt{\mu_E} \cos i \tag{1}$$

$$\dot{\omega}(a,i) = \frac{3}{2} J_2 \frac{R_E^2}{a^{\frac{7}{2}}} \sqrt{\mu_E} \left(2 - \frac{5}{2} \sin^2 i \right) \tag{2}$$

$$\dot{M}(a,i) = \frac{3}{2} J_2 \frac{R_E^2}{a^{\frac{7}{2}}} \sqrt{\mu_E} \left(1 - \frac{3}{2} \sin^2 i \right) + \sqrt{\frac{\mu_E}{a^3}} \tag{3}$$

In the relationships (1)-(3) (holding for circular orbits) R_E, μ_E, and J_2 are the Earth radius, planetary constant, and oblateness coefficient, whereas a and i are the orbit semi-major axis (SMA) and inclination, respectively. Due to (1)-(3), if Ω_0, ω_0, and M_0 are the initial values (at $t_0 = 0$) of Ω, ω, and M, the related time histories are linear with time. However, for circular orbits only the argument of latitude $\theta = \omega + M$ is meaningful because the perigee is not defined. As a result, the time-varying orbital elements $\Omega(t)$ and $\theta(t)$ are given by:

$$\Omega(t) = \Omega_0 + \dot{\Omega}(a,i)t \tag{4}$$

$$\theta(t) = \theta_0 + \dot{\theta}(a,i)t \tag{5}$$

where $\dot{\theta}(a,i) = \dot{\omega}(a,i) + \dot{M}(a,i)$ and $\theta_0 = \omega_0 + M_0$. All the satellites are assumed to have identical inclination and SMA (or altitude H for circular orbits) in order to avoid differential actions

by J_2 perturbation on each of them. This circumstance would cause a substantial alteration of the performance attainable by the constellation.

An orbit is termed repeating when phased with Earth rotation, i.e. when the trajectory ground track is periodically repeated. This occurs if the satellite completes N_t orbits in m nodal days:

$$mD_n(a,i) = N_t T_n(a,i) \tag{6}$$

In (6): $T_n = 2\pi/\dot{\theta}$ is the nodal orbital period (i.e., the time interval between two consecutive ascending node crossings), and $D_n = 2\pi/(\omega_E - \dot{\Omega})$ is the nodal day (i.e. the time required for the Earth to make a complete rotation with respect to the orbital plane; ω_E denotes the Earth rotation rate). Both T_n and D_n depend on the orbit SMA, a, and inclination, i. This fact implies that the ratio $r_t = N_t / m$, which represents the number of orbits per nodal day, depends on a and i. Conversely, once N_t and m are specified, the orbit inclination can be expressed as a function of a through (6). In this research, five possible choices for (N_t, m) are considered, corresponding to different ranges of altitudes as the orbit inclination varies from 0 to 90 degrees. These ranges are reported in Table 1, with the respective values of N_t and m.

Table 1: Minimum and maximum altitude, H_{min} and H_{max}, depending on (N_t, m)

N_t	m	r_t	H_{min} (km)	H_{max} (km)
14	1	14	812.4	874.5
43	3	14.333	696.1	761.4
29	2	14.5	639.6	706.5
44	3	14.667	584.1	652.6
15	1	15	476.0	547.9

Ground tracks of satellites in circular repeating orbits exhibit a typical reticular shape. Two types of grid exist: the first kind (named grid α) has coincident ascending and descending equatorial crossings, unlike the second one (named grid β). This feature depends on the sum

$(N_t + m)$, as proved in Appendix 2: grid α corresponds to $(N_t + m)$ even, grid β to $(N_t + m)$ odd. Figures 1 and 2 illustrate two examples of these two types of repeating ground tracks.

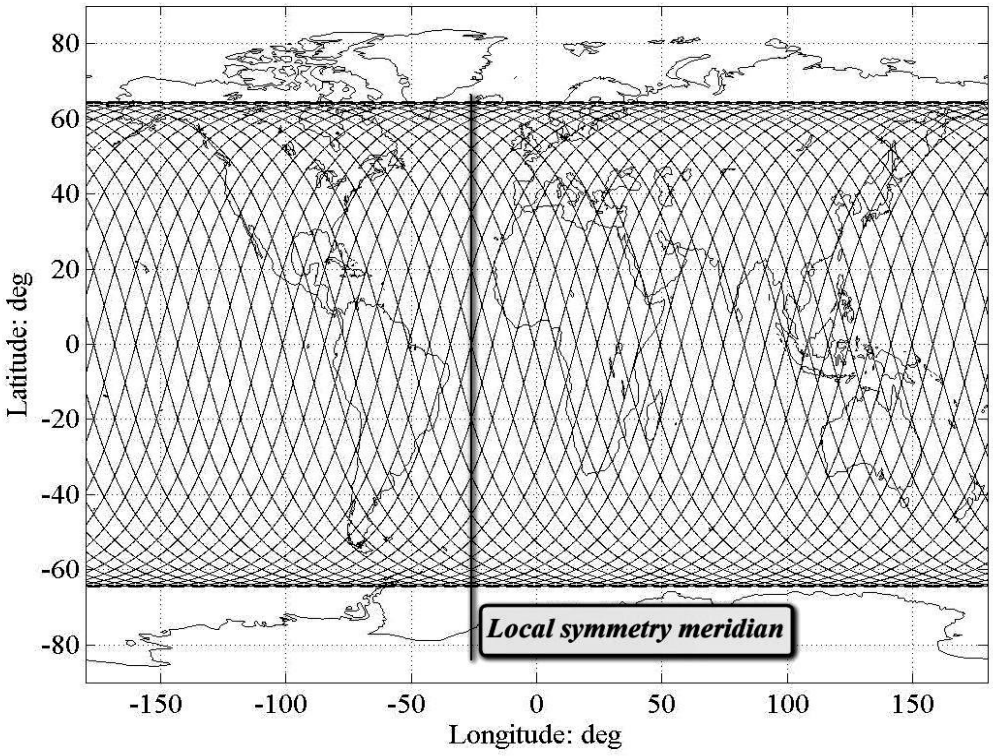

Fig. 1: Grid α. Ground track of a repeating satellite $(N_t = 43,\ m = 3)$

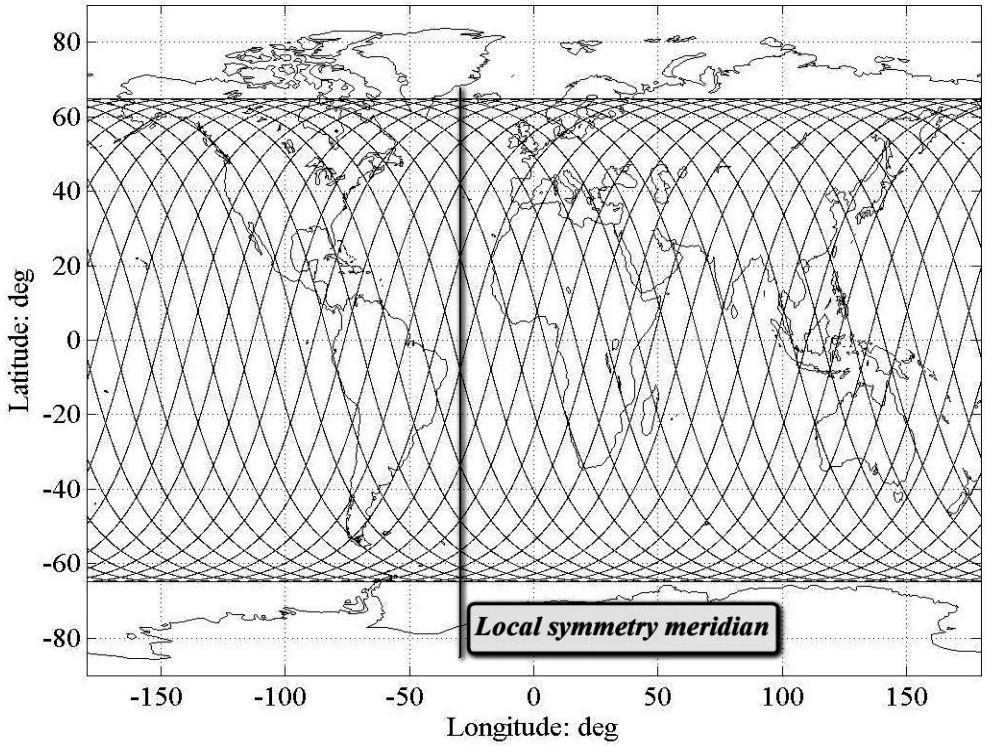

Fig. 2: Grid β. Ground track of a repeating satellite $\left(N_t = 29,\ m = 2\right)$

From the inspection of Figures 1 and 2 it emerges that each grid presents local symmetry with respect to meridians passing through grid interception points (two of these meridians are portrayed in Figures 1 and 2). Basically, this feature is related to the circularity of the orbits and will be employed in Section 3. Moreover, due to the circularity of the orbits again, the total duration of visibility for a single satellite is proportional to the geometrical length of the visible ground track arcs, corresponding to the satellite instantaneous positions from which the entire target area is visible.

3. Optimal orbital elements for a single satellite

Constellation design is aimed at ensuring some visibility properties of a target region from the satellites that form the constellation. The target area is assumed to be delimited in longitude ($\lambda_l \le \lambda \le \lambda_u$) and latitude ($\phi_l \le \phi \le \phi_u$), and is considered visible from a single satellite if all the points belonging to this area are in view with an elevation angle γ greater than the minimum value γ_{min}. This minimum value is related to the onboard instrumentation. In this study, the following values of γ_{min} are assumed for two types of constellation (associated to different onboard instruments):

- ❒ constellation for telecommunication services: $\gamma_{min} = 5$ deg
- ❒ constellation for monitoring services: $\gamma_{min} = 40$ deg

With reference to ground tracks of repeating satellites, the longitudinal separation between two adjacent (generally not consecutive) ascending nodes is $2\pi/N_t$, and this is also the angular separation of longitudinal repetition at all latitudes. Hence, when the maximum duration of visibility occurs for a specified target region (associated to the average longitude $\lambda_{av} = 0.5(\lambda_l + \lambda_u)$ and to the average latitude $\phi_{av} = 0.5(\phi_l + \phi_u)$) the same maximum duration also occurs for other regions with the same longitudinal and latitudinal extension. Due to the basic properties of repeating ground tracks of circular orbits, these regions are simply shifted in longitude and two cases can be distinguished:

1. $(N_t + m)$ even (grid α): all the regions associated to $(\lambda_{av} + 2k\pi/N_t, \pm\phi_{av})$, with $k = 0,..., N_t - 1$, are characterized by the same total duration of visibility
2. $(N_t + m)$ odd (grid β): all the regions associated to $(\lambda_{av} + 2k\pi/N_t, \phi_{av})$ and $(\lambda_{av} + \pi/N_t + 2k\pi/N_t, -\phi_{av})$, with $k = 0,..., N_t - 1$, are characterized by the same total duration of visibility

Now, what will be demonstrated is that, for a given orbit, the total duration of visibility, $T_{tot}^{(vis)}$, has an extremum when the visible ground track is symmetric with respect to the central meridian of the target area, as shown in Fig. 3(c). This property can be deduced in the following fashion:

- let the central meridian be a line of local symmetry for the repeating ground track; this circumstance implies that also the visible ground track arcs are symmetrical with respect to the central meridian of the target region, as in Fig. 3(c)
- the symmetrical situation portrayed in Fig. 3(c) is assumed to correspond to a specific value $\bar{\Omega}_0$ of the initial RAAN and to a visibility duration $T_{tot,extr}^{(vis)}$
- if two displacements are imposed on $\bar{\Omega}_0$ $\left((a).\ \Omega_{0a} = \bar{\Omega}_0 + \delta,\ (b).\ \Omega_{0b} = \bar{\Omega}_0 - \delta\right)$, the resulting grids are shifted towards East and towards West by the same angle (Figures 3(a) and 3(b))
- the total length of the visible ground track arcs is the same in these two situations (illustrated in Figures 3(a) and 3(b)), so also the total duration of visibility is the same and is equal to $\left(T_{tot,extr}^{(vis)} + \Delta T^{(vis)}\right)$ in both situations

- as a consequence, depending on $\Delta T^{(vis)}$, the symmetric condition corresponds to a maximum or to a minimum for the total visibility: if $\Delta T^{(vis)} > 0$, $T_{tot}^{(vis)}$ has a minimum for $\Omega_0 = \bar{\Omega}_0$, otherwise, if $\Delta T^{(vis)} < 0$, $T_{tot}^{(vis)}$ has a maximum

As a result, all the values of Ω_0 yielding such a symmetry must be checked in order to find the optimal value, which maximizes $T_{tot}^{(vis)}$.

Due to the geometric features of the grids α and β, the symmetry condition can be examined making reference to the equatorial region of the ground tracks. As a matter of fact, if at the equator the ground track is symmetric with regard to the central meridian of the target area, then this symmetry also holds for the visible ground track arcs. Ground tracks can be shifted towards East or West by simply varying the initial RAAN, Ω_0, so the simplest way of guaranteeing such a symmetry consists in choosing $\theta_0 = 0$ (satellite at the ascending node for $t = t_0 = 0$), and Ω_0 between the following two values:

1. For grid α ($\left(N_t + m\right)$ even, Fig. 4(a)):

$$\text{A. } \Omega_0 = \theta_{g0} + \lambda_{av} - \frac{\pi}{N_t} \qquad \text{or} \qquad \text{B. } \Omega_0 = \theta_{g0} + \lambda_{av} \tag{7}$$

2. For grid β ($\left(N_t + m\right)$ odd, Fig. 4(b)):

$$\text{A. } \Omega_0 = \theta_{g0} + \lambda_{av} - \frac{\pi}{2N_t} \qquad \text{or} \qquad \text{B. } \Omega_0 = \theta_{g0} + \lambda_{av} + \frac{\pi}{2N_t} \tag{8}$$

where θ_{g0} is the Greenwich initial sidereal time. It is worth mentioning that all the optimal values of Ω_0 are repeated with periodicity equal to $2\pi/N_t$.

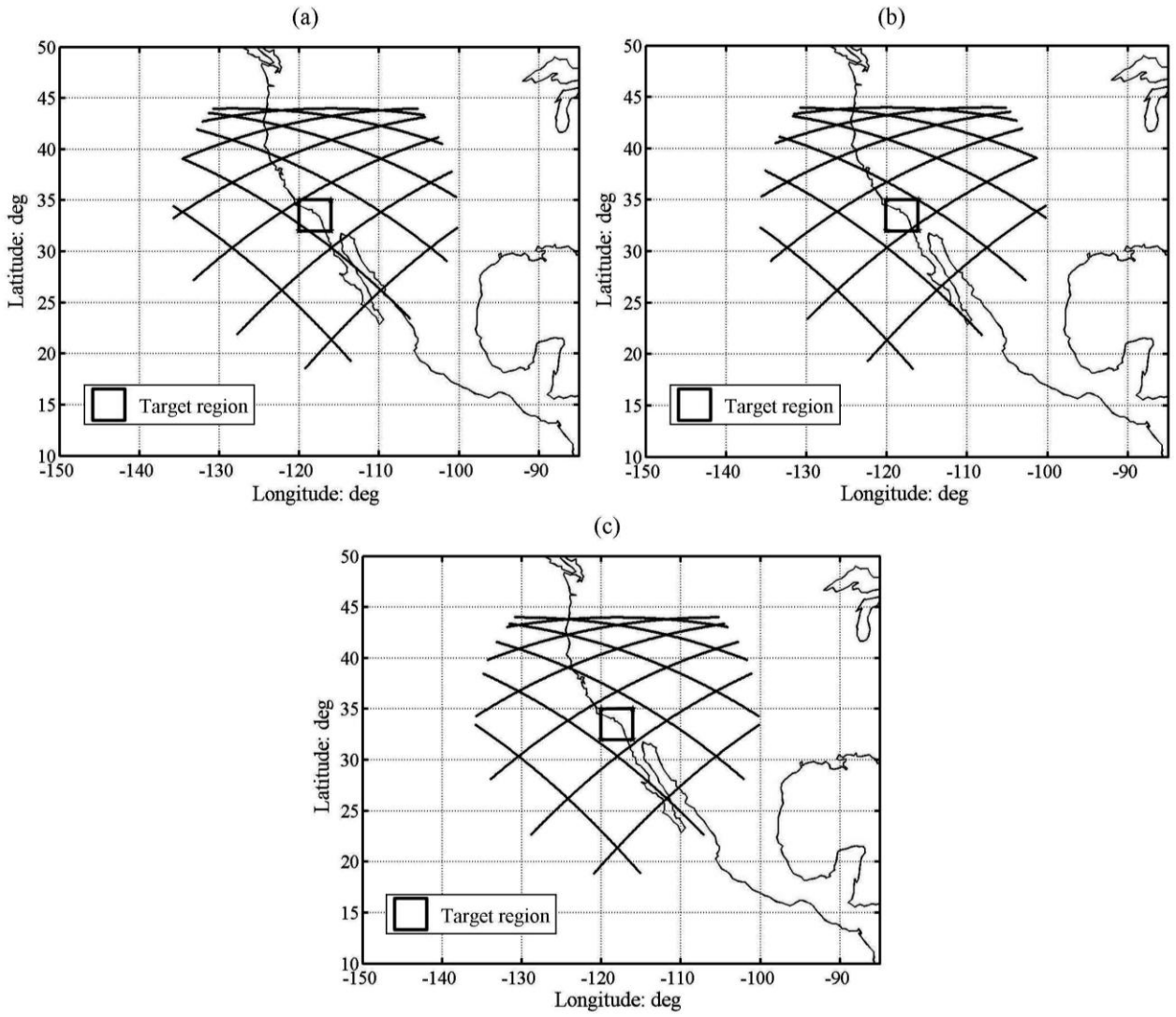

Fig. 3: Visible ground tracks corresponding to different values of Ω_0. (a), (b) Asymmetric visible ground tracks. (c) Symmetric visible ground track

If N_t and m are specified, for each of the two possible values of Ω_0 a numerical investigation on the SMA is performed with the purpose of maximizing the total duration of visibility. This search is based on the following points:

- the target region is in view if and only if the following points are visible at a time: $P_1(\lambda_l, \phi_l)$, $P_2(\lambda_l, \phi_u)$, $P_3(\lambda_u, \phi_u)$, and $P_4(\lambda_u, \phi_l)$
- for each value of *a*, *i* is calculated through (6), and the time-dependent East, North, and up coordinates $((x_k, y_k, z_k),\ k = 1,\ 2,\ 3,\ 4)$ in the local frame centered in P_k $(k = 1,2,3,4)$ are calculated

- the satellite is in view from P_k if the following relationship holds:

$$\tan\gamma = \frac{z_k(t)}{\sqrt{\left[x_k(t)\right]^2 + \left[y_k(t)\right]^2}} \geq \tan\gamma_{min} \tag{9}$$

- each time interval of visibility is such that (9) holds for all the four points $\{P_k\}_{k=1,2,3,4}$: this is the basic condition that allows determining the total duration of visibility
- finally, the optimal value of the SMA *a*, which maximizes the total duration of visibility, is selected, and the optimal value of the orbit inclination *i* is calculated through (6)

These steps lead to determining the optimal values of all the orbital parameters for the first satellite belonging to the constellation. Definitely, the maximization of the total duration of visibility, achieved for the first satellite through the optimal selection of its orbital elements, leads to the identification of a specific ground track.

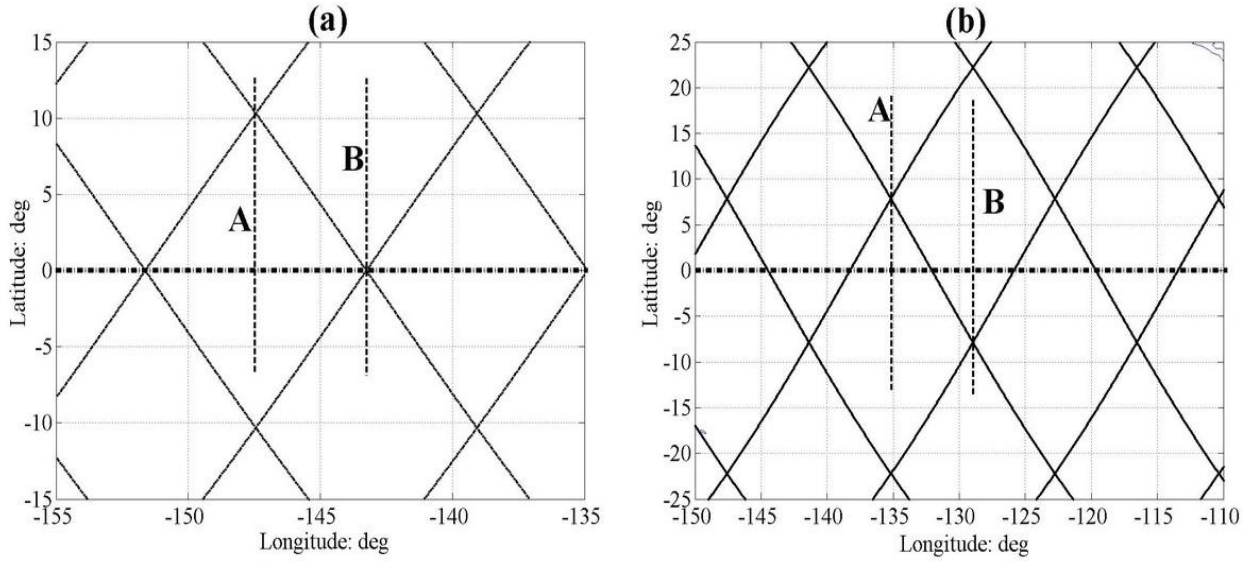

Fig. 4: Equatorial regions of repeating circular ground tracks: (a) grid α; (b) grid β

It is desirable that all the remaining satellites of the constellation preserve the same visibility properties. To do this, their orbits must be associated to the same ground track, i.e. their motion relative to the Earth surface must be identical to that of the first satellite, albeit delayed. Section 4 addresses the central issue of determining the optimal delays that characterize the relative motion of the constellation satellites.

4. Strategy for constellation design

This section is focused on the original strategy that will be employed to identify optimal constellation configurations, with reference to two distinct (conflicting) requirements:

- Requirement A: maximize the maximum coverage, i.e. the maximum continuous time interval of visibility of the target area from the constellation $\left(\max \mathrm{MCov}\right)$
- Requirement B: minimize the maximum revisit time, representing the maximum time interval when the target region is not visible from any satellite $\left(\min \mathrm{MGap}\right)$

The target area is considered in view when it is visible from at least one satellite. As repeating orbits have been assumed for the constellation satellites, the mentioned requirements can be referred to the period of repetition.

4.1. Visibility function

After selecting the orbit SMA, inclination, and initial RAAN, for a single satellite all the intervals of visibility (termed "white segments" hence forward) and the gaps of non-visibility (termed "black segments") can be determined. An auxiliary function, named "visibility function", depending on the actual time t and directly related to these segments, can be introduced as:

$$V_1(t)=\begin{cases}0, & \text{if the satellite 1 is not visible at instant t}\\ 1, & \text{if the satellite 1 is visible at instant t}\end{cases} \qquad \left(0\le t\le T \;\square\; N_t T_n = mD_n\right) \quad (10)$$

Now, let n be the number of white segments. $\left\{t_l^{(in)}\right\}_{l=1,\ldots,n}$ and $\left\{t_l^{(out)}\right\}_{l=1,\ldots,n}$ respectively identify the starting and the terminal point of each of them. Then, t_{0l} and T_l are defined by:

$$t_{0l}=0.5\left(t_l^{(out)}+t_l^{(in)}\right) \qquad T_l=t_l^{(out)}-t_l^{(in)} \qquad \left(l=1,\ldots,n\right) \qquad (11)$$

They respectively represent the medium point and the length of each white segment. Through (11), $V_1(t)$ can be written as:

$$V_1(t)=\sum_{l=1}^{n}\mathrm{rect}_{T_l}\left(t-t_{0l}\right) \qquad \text{where} \qquad \mathrm{rect}_B(t)=\begin{cases}0 & \text{if} \quad |t|>B/2\\ 1 & \text{if} \quad |t|\le B/2\end{cases} \qquad \left(B>0\right) \qquad (12)$$

Due to periodicity, black and white segments are repeated for $t>T$, so (10) and (12) can be formally extended to $V_1^P(t)$:

$$V_1^P(t)=\sum_{k=-\infty}^{\infty}V_1\left(t-kT\right)=\sum_{k=-\infty}^{\infty}\left[\sum_{l=1}^{n}\mathrm{rect}_{T_l}\left(t-kT-t_{0l}\right)\right] \quad \text{with} \quad t\ge 0 \quad (13)$$

Then, at the time $t = \tau_{1,2}$ a second satellite (with SMA and inclination identical to the first) is supposed to cross the equator (from South to North) at the same point relative to Earth surface. The related functions $V_2^P(t)$ and $V_2(t)$ are respectively $V_1^P(t)$ and $V_1(t)$ shifted forward by $\tau_{1,2}$:

$$V_2^P(t) = V_1^P(t - \tau_{1,2}) = \sum_{k=-\infty}^{\infty} V_2(t - kT) = \sum_{k=-\infty}^{\infty} V_1(t - \tau_{1,2} - kT), \qquad t \geq 0 \qquad (14)$$

The overlapping of these visibility functions ($V_1^P(t)$ and $V_2^P(t)$) is useful for the identification of the maximum coverage (MCov) and of the maximum gap (MGap), as illustrated in Fig. 5 for a pair of satellites whose visibility functions partially overlap.

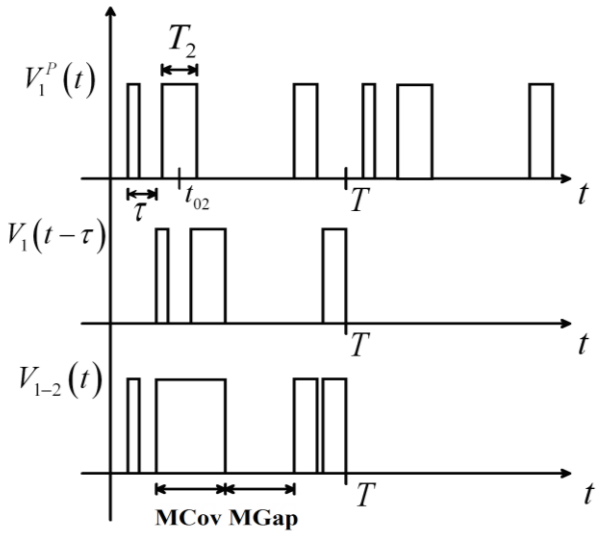

Fig. 5: Overlapping of visibility functions (schematic example)

4.2. Description of the method

With reference to a two-satellite constellation, a suitable way of increasing the continuous coverage duration and simultaneously reducing the gap duration follows two basic principles:

A. Avoid the overlapping of two white segments ("non-overlapping condition")
B. choose the delay $\tau_{1,2}$ such that two white segments have a single adjacency point ("adjacency condition")

According to this approach, the target location will be in view from a single satellite at a time and, in addition, an instant will exist when the first satellite goes out of visibility and the second one

goes into visibility (or vice versa). Yet, the adjacency condition is not strictly necessary for the purpose of minimizing the maximum gap. On the contrary, a globally "sparse" and homogeneous disposal of white segments can reveal suitable in such a situation. This sparse disposal can be achieved by inserting a white segment of the second satellite just in the middle of a black segment of the first. This fact means that a visible pass of the second satellite is inserted just mid-way between two consecutive passes of the first. As an immediate consequence, *sparseness delays* are given by $\left(\tau_{1,2}^{(h)}+\tau_{1,2}^{(h+1)}\right)\Big/2 \ \left(h=1,...,N_{adj}^{(C)}-1\right)$, where $\tau_{1,2}^{(h)}$ and $\tau_{1,2}^{(h+1)}$ are two consecutive *adjacency delays* and $N_{adj}^{(C)}$ is their total number. Fig. 6 shows a schematic example of the sparse disposal of a white segment of the satellite 2 between two white segments of the satellite 1: a right or left shift of the segment C increases the maximum gap.

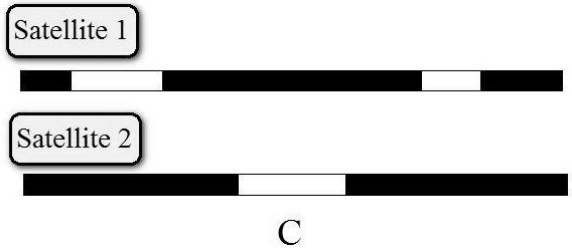

Fig. 6: Example of sparse disposition of a white segment of the satellite 2 between two of the satellite 1

Once $\tau_{1,2}$ has been determined, the visibility function $V_{1-2}^{P}(t)$ can be generated, and identifies the white segments and the black segments for the system composed of the two satellites. With the above assumption A, $V_{1-2}^{P}(t)$ is given by:

$$V_{1-2}^{P}(t)=V_{1}^{P}(t)+V_{2}^{P}(t)=V_{1}^{P}(t)+V_{1}^{P}\left(t-\tau_{1,2}\right) \tag{15}$$

The described strategy can be very easily extended to consider 4, 8 or 16 satellites. $V_{1-2}^{P}\left(t-\tau_{2,4}\right)$ represents a second couple of satellites, delayed by $\tau_{2,4}$ with respect to the first. Hence, for the system composed of the four satellites the visibility function $V_{1-4}^{P}(t)$ can be written as follows:

$$V_{1-4}^{P}(t)=V_{1-2}^{P}(t)+V_{3-4}^{P}(t)=V_{1-2}^{P}(t)+V_{1-2}^{P}\left(t-\tau_{2,4}\right) \tag{16}$$

Obviously, for 8 and 16 satellites similar relationships hold.

The above non-overlapping assumption A forces the following integral to vanish:

$$R_{1-2}\left(\tau_{1,2}^{(h)}\right)=\int_{-\infty}^{\infty}V_1^P\left(t\right)V_2\left(t\right)dt=\int_{-\infty}^{\infty}V_1^P\left(t\right)V_1\left(t-\tau_{1,2}^{(h)}\right)dt=0 \qquad \left(h=1,...,s\right) \qquad (17)$$

All allowed delays $\left\{\tau_{1,2}^{(h)}\right\}_{h=1,...,s}$ must annihilate $R_{1-2}\left(\xi\right)$, which can be seen as a correlation function depending on $\xi=-\tau_{1,2}^{(h)}$. The adjacency condition holds if, in addition to the condition (17), $R_{1-2}\left(\tau_{1,2}\right)\neq 0$ for $\tau_{1,2}=\tau_{1,2}^{(h)}+\varepsilon$ or $\tau_{1,2}=\tau_{1,2}^{(h)}-\varepsilon$ (where ε is an arbitrary small, positive number). Due to periodicity of the visibility functions, the correlation function (17) is repeated for $t>T$, so the analysis can be made over the interval $\left[0,T\right]$. The correlation integral is composed of six terms and in $\left[0,T\right]$ has the following expression, derived in [14]:

$$\begin{aligned}R_{1-2}\left(\tau_{1,2}\right)=&\sum_{\substack{\nu=1,...n\\ \sigma=\nu+1,...,n}}\left\{\underset{T_\nu,T_\sigma}{\operatorname{trapz}}\left[\tau_{1,2}-\left(T+t_{0\nu}-t_{0\sigma}\right)\right]+\underset{T_\nu,T_\sigma}{\operatorname{trapz}}\left[\tau_{1,2}-\left(T+t_{0\sigma}-t_{0\nu}\right)\right]\right\}+\\ &+\sum_{l=1}^{n}\left\{T_l\underset{T_l}{\operatorname{tri}}\left(\tau_{1,2}\right)+T_l\underset{T_l}{\operatorname{tri}}\left(\tau_{1,2}-T\right)\right\}+\sum_{\substack{\nu=1,...n\\ \sigma=\nu+1,...,n}}\left\{\underset{T_\nu,T_\sigma}{\operatorname{trapz}}\left[\tau_{1,2}-\left(t_{0\nu}-t_{0\sigma}\right)\right]+\underset{T_\nu,T_\sigma}{\operatorname{trapz}}\left[\tau_{1,2}-\left(t_{0\sigma}-t_{0\nu}\right)\right]\right\}\end{aligned} \qquad (18)$$

where

$$\underset{B}{\operatorname{tri}}\left(\xi\right)=\begin{cases}1-\dfrac{\left|\xi\right|}{B} & \text{if} \quad 0\le\left|\xi\right|\le B\\ 0 & \text{if} \quad \left|\xi\right|\ge B\end{cases} \qquad \text{and} \qquad \underset{T_\nu,T_\sigma}{\operatorname{trapz}}\left(\xi\right)=\frac{T_\nu+T_\sigma}{2}\underset{\frac{T_\nu+T_\sigma}{2}}{\operatorname{tri}}\left(\xi\right)-\frac{\left|T_\nu-T_\sigma\right|}{2}\underset{\frac{\left|T_\nu-T_\sigma\right|}{2}}{\operatorname{tri}}\left(\xi\right) \qquad (19)$$

The analytic expression (18) of the correlation function is extremely useful since both accuracy and computational efficiency in finding all adjacency delays are greatly improved. In addition, the function $R_{1-2}\left(\tau_{1,2}\right)$ is symmetric with respect to $\tau_{1,2}=T/2$, so the allowed delays $\left\{\tau_{1,2}^{(h)}\right\}$ can be searched in the interval $\left[0,T/2\right]$: this circumstance further enhances effectiveness.

4.3. Algorithmic search for allowed time delays

The fulfillment of the requirements A and B can be achieved after comparing all the constellation configurations associated to the zeros of the correlation function. Each configuration corresponds to a sequence of time delays. The algorithmic search of all the allowed time delays is addressed in this subsection.

First, from the inspection of the expression (18) of the correlation function $R_{1-2}(\tau_{1,2})$, it turns out that it is composed of several (partially) overlapping terms. Allowed delays must annihilate all of them. A necessary condition for the existence of zeros of $R_{1-2}(\tau_{1,2})$ is that

$$\max_l(T_l) < T/2 \tag{20}$$

otherwise no value for $\tau_{1,2}$ exists that annihilates both the third and the fourth term in (18). Yet, the condition (20) is always met in applicative situations regarding LEO constellations, because the duration of the visible passes is much shorter than the period of repetition of the satellite orbits.

As a preliminary step, for the sake of simplicity, the auxiliary matrices $\boldsymbol{\delta},\ \boldsymbol{\beta},\ \boldsymbol{\alpha}\ \ (n\times n)$ are introduced. Their elements are defined as follows:

$$\delta_{\nu\sigma} = t_{0\nu} - t_{0\sigma} \qquad \beta_{\nu\sigma} = T_\nu + T_\sigma \qquad \alpha_{\nu\sigma} = \delta_{\nu\sigma} + \beta_{\nu\sigma} \tag{21}$$

An immediate consequence of (21) is that: $\alpha_{\sigma\nu} = \beta_{\sigma\nu} + \delta_{\sigma\nu} = \beta_{\nu\sigma} - \delta_{\nu\sigma}$. Moreover, the intervals of admissibility for $\tau_{1,2}$ are such that every single term in (18) vanishes. These intervals are listed below:

1. $\underset{T_\nu,T_\sigma}{\text{trapz}}\left[\tau_{1,2} - \left(T + t_{0\nu} - t_{0\sigma}\right)\right]:\quad \left\{\tau_{1,2} \ge T + \alpha_{\nu\sigma}\right\} \cup \left\{\tau_{1,2} \le T - \alpha_{\sigma\nu}\right\} \quad \forall \begin{cases}\nu = 1,\ldots,n\\ \sigma = \nu+1,\ldots,n\end{cases}$ (22)

2. $\underset{T_\nu,T_\sigma}{\text{trapz}}\left[\tau_{1,2} - \left(T + t_{0\sigma} - t_{0\nu}\right)\right]:\quad \left\{\tau_{1,2} \le T - \alpha_{\nu\sigma}\right\} \quad \forall \begin{cases}\nu = 1,\ldots,n\\ \sigma = \nu+1,\ldots,n\end{cases}$ (23)

3. $T_l \underset{T_l}{\text{tri}}\left(\tau_{1,2}\right):\quad \left\{\tau_{1,2} \ge T_l\right\}\ \forall\ l = 1,\ldots,n \quad \text{so} \quad \tau_{1,2} \ge \max_l\left(T_l\right)$ (24)

4. $T_l \underset{T_l}{\text{tri}}\left(\tau_{1,2} - T\right):\quad \left\{\tau_{1,2} \le T - T_l\right\}\ \forall\ l = 1,\ldots,n \quad \text{so} \quad \tau_{1,2} \le T - \max_l\left(T_l\right)$ (25)

5. $\underset{T_\nu,T_\sigma}{\text{trapz}}\left[\tau_{1,2} - \left(t_{0\nu} - t_{0\sigma}\right)\right]:\quad \left\{\tau_{1,2} \ge \alpha_{\nu\sigma}\right\} \quad \forall \begin{cases}\nu = 1,\ldots,n\\ \sigma = \nu+1,\ldots,n\end{cases}$ (26)

6. $\underset{T_\nu,T_\sigma}{\text{trapz}}\left[\tau_{1,2} - \left(t_{0\sigma} - t_{0\nu}\right)\right]:\quad \left\{\tau_{1,2} \ge \alpha_{\sigma\nu}\right\} \cup \left\{\tau_{1,2} \le -\alpha_{\nu\sigma}\right\} \quad \forall \begin{cases}\nu = 1,\ldots,n\\ \sigma = \nu+1,\ldots,n\end{cases}$ (27)

It is worth mentioning that these intervals must be included between 0 and *T* to preserve significance.

Now, candidate adjacency and sparseness delays can be determined through the following steps:

1. The set of the *candidate adjacency delays* is composed of all the extreme values delimiting the intervals of admissibility; their number is denoted with $N_{adj}^{(C)}$. In short, the following scheme can be followed:

$$\begin{array}{lllll} \text{if} & \alpha_{\kappa\rho} < 0 \;\Rightarrow & \tau_{1,2} = -\alpha_{\kappa\rho} & \text{and} & \tau_{1,2} = T + \alpha_{\kappa\rho} \\ \text{if} & \alpha_{\kappa\rho} > 0 \;\Rightarrow & \tau_{1,2} = \alpha_{\kappa\rho} & \text{and} & \tau_{1,2} = T - \alpha_{\kappa\rho} \end{array} \quad \text{with} \quad \begin{cases} \kappa = 1,...,n \\ \rho = 1,...,n \end{cases} \tag{28}$$

$$\tau_{1,2} = \max_{l}\left(T_l\right) \quad \text{and} \quad \tau_{1,2} = T - \max_{l}\left(T_l\right) \tag{29}$$

2. Once all candidate adjacency delays have been determined, the set of the *candidate sparseness delays* includes the following values:

$$\tau_{1,2} = \frac{\tau_{1,2}^{(h)} + \tau_{1,2}^{(h+1)}}{2} \qquad \left(h = 1,..., N_{adj}^{(C)} - 1\right) \tag{30}$$

where $\tau_{1,2}^{(h)}$ and $\tau_{1,2}^{(h+1)}$ are two consecutive adjacency delays.

Definitely, the algorithmic search of *allowed delays* can be summarized as follows:

(a) all candidate adjacency delays are calculated by means of (28), (29) and

(b) all candidate sparseness delays are calculated through (30) once candidate adjacency delays are determined

(c) for each candidate delay, if all the conditions (22)-(27) hold, the *candidate* delay becomes an *allowed* delay (which does not generate overlapping among visibility functions)

If the maximization of MCov is asked for (Requirement A), the point (b) can be skipped, since the sparseness condition is not compatible with increasing the maximum duration of the continuous coverage.

All the above steps and considerations can be repeated making reference to $\tau_{2,4}$, $\tau_{4,8}$, $\tau_{8,16}$ when 4, 8, and 16 satellites are considered.

Basically, discrete sets of allowed delays exist. Let s be the number of all the allowed delays $\left\{\tau_{1,2}^{(h)}\right\}_{h=1,...,s}$ that generate $V_{1-2}^{P}(t)$; for each $\tau_{1,2}^{(h)}$, the set $\left\{\tau_{2,4}^{(h,j)}\right\}_{j=1,...,s_h}$ of allowed delays that generate $V_{1-4}^{P}(t)$ can be determined. In the same way, for each $\tau_{2,4}^{(h,j)}$, the set $\left\{\tau_{4,8}^{(h,j,z)}\right\}_{z=1,...,s_{hj}}$ of allowed delays generating $V_{1-8}^{P}(t)$ can be found, and so on. This process results in the generation of a typical tree structure, which includes all the allowed time delays. The total number of configurations N_w for constellations of w satellites is given by:

$$N_2 = s \qquad N_4 = \sum_{h=1}^{s} s_h \qquad N_8 = \sum_{h=1}^{s}\sum_{j=1}^{s_h} s_{hj} \tag{31}$$

4.4. Constellation orbital elements

The determination of the optimal time delays allows deriving the orbital elements of all the satellites that form the constellation. As discussed in Section 3, at the initial time the first satellite is assumed to be at the ascending node, i.e. $\theta_{01} = 0$. Its initial RAAN, Ω_{01}, is selected through the method described in the same section. All the remaining satellites are associated to the same ground track, i.e. their motion relative to the Earth surface must be identical to that of the first satellite. If the second satellite is delayed by $\tau_{1,2}$ with respect to the first, then it must be at the ascending node at $t = \tau_{1,2}$; this circumstance implies that

$$\theta_2\left(\tau_{1,2}\right) = \theta_{02} + \dot{\theta}(a,i)\tau_{1,2} = 2\pi \qquad \text{so} \qquad \theta_{02} = 2\pi - \dot{\theta}(a,i)\tau_{1,2} \tag{32}$$

In addition, the second ground track preserves the same property of local symmetry with respect to the target area if the following relationship holds:

$$\Omega_2\left(\tau_{1,2}\right) - \left[\theta_g\left(\tau_{1,2}\right) + \lambda_{av}\right] = \Omega_{01} - \left[\theta_{g0} + \lambda_{av}\right] \tag{33}$$

where $\theta_g\left(\tau_{1,2}\right) = \theta_{g0} + \omega_E \tau_{1,2}$ is the Greenwich sidereal time at $t = \tau_{1,2}$. After introducing (4), (33) becomes:

$$\Omega_{02} = \Omega_{01} + \left[\omega_E - \dot{\Omega}(a,i)\right]\tau_{1,2} \tag{34}$$

If (32) and (34) hold, the two satellites cross the equator exactly at the same point relative to the Earth surface and this circumstance ensures that they are associated to the same ground track.

The orbital elements of the remaining satellites can be obtained by employing the corresponding time delays with respect to the first satellite in (32) and (34), instead of $\tau_{1,2}$. These delays are straightforward to deduce and for satellites 3 through 8 are given by:

$$\Delta t_3 = \tau_{2,4},\ \Delta t_4 = \tau_{2,4} + \tau_{1,2},\ \Delta t_5 = \tau_{4,8},\ \Delta t_6 = \tau_{4,8} + \tau_{1,2},\ \Delta t_7 = \tau_{4,8} + \tau_{2,4},\ \Delta t_8 = \tau_{4,8} + \tau_{2,4} + \tau_{1,2} \tag{35}$$

5. Optimal constellation configurations

The method described in Section 4 is applied to several cases of possible practical interest. Four regions have been selected as target areas:

- Region 1: $\lambda_l = -120$ deg and $\lambda_u = -116$ deg; $\phi_l = 32$ deg and $\phi_u = 35$ deg
- Region 2: $\lambda_l = -46$ deg and $\lambda_u = -42$ deg; $\phi_l = 60$ deg and $\phi_u = 63$ deg
- Region 3: $\lambda_l = -100$ deg and $\lambda_u = -98$ deg; $\phi_l = 19$ deg and $\phi_u = 20$ deg
- Region 4: $\lambda = -1$ deg and $\lambda_u = 1$ deg; $\phi_l = 51$ deg and $\phi_u = 52$ deg

Region 1 corresponds to a relevant part of California, including the entire metropolitan area of Los Angeles and San Diego. Region 2 is located on the southern part of Greenland. Region 3 includes the metropolitan area of Mexico City, and, finally, region 4 corresponds to the metropolitan area of London.

The performance attained by four- and eight-satellite constellations is summarized in Tables 2 and 3, which refers to different choices of N_t and m (resulting in different altitudes of the satellite orbits), and to the basic requirements A and B. The performance of monitoring constellations turns out to be inferior in all cases, due to the higher elevation angle required for visibility, albeit regions 3 and 4 are smaller in extension with respect to regions 1 and 2. Some constellation configurations and visibility spots are portrayed in Figures 7-10. In all cases, the maximum continuous coverage of a target corresponds to the set of the minimum allowed time delays yielding adjacent and non-overlapping visibility functions. This is a very general and foreseeable result for all location latitudes. It consists in concatenating the widest time intervals of visibility of all the satellites, whose related visibility spots assume the aspect shown in Fig. 8.

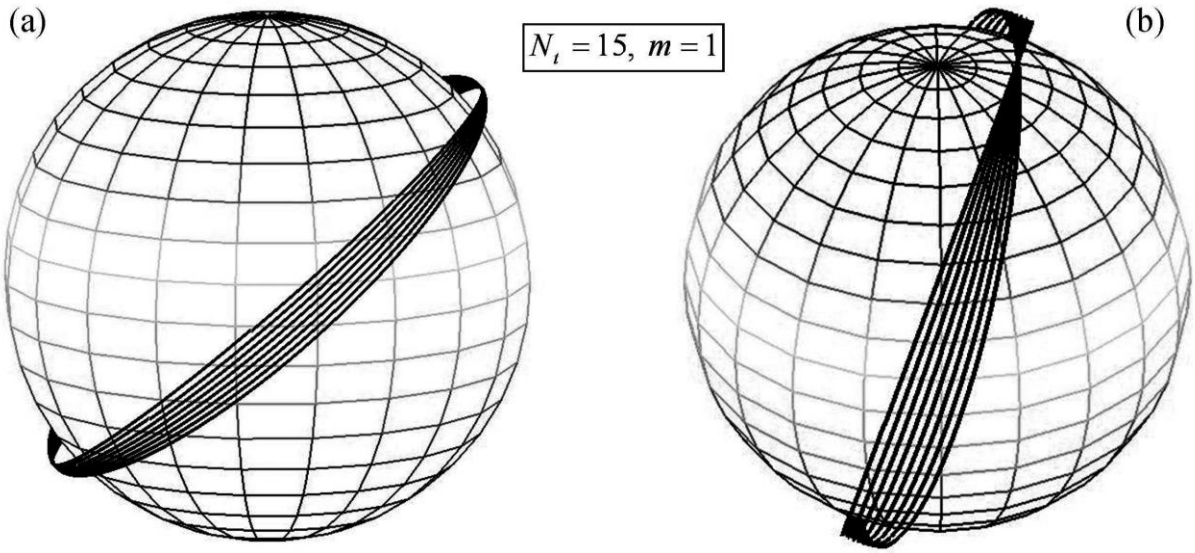

Fig. 7: Two 8-satellite telecommunication constellations optimal with respect to requirement A, with reference to region 1 (a) and to region 2 (b)

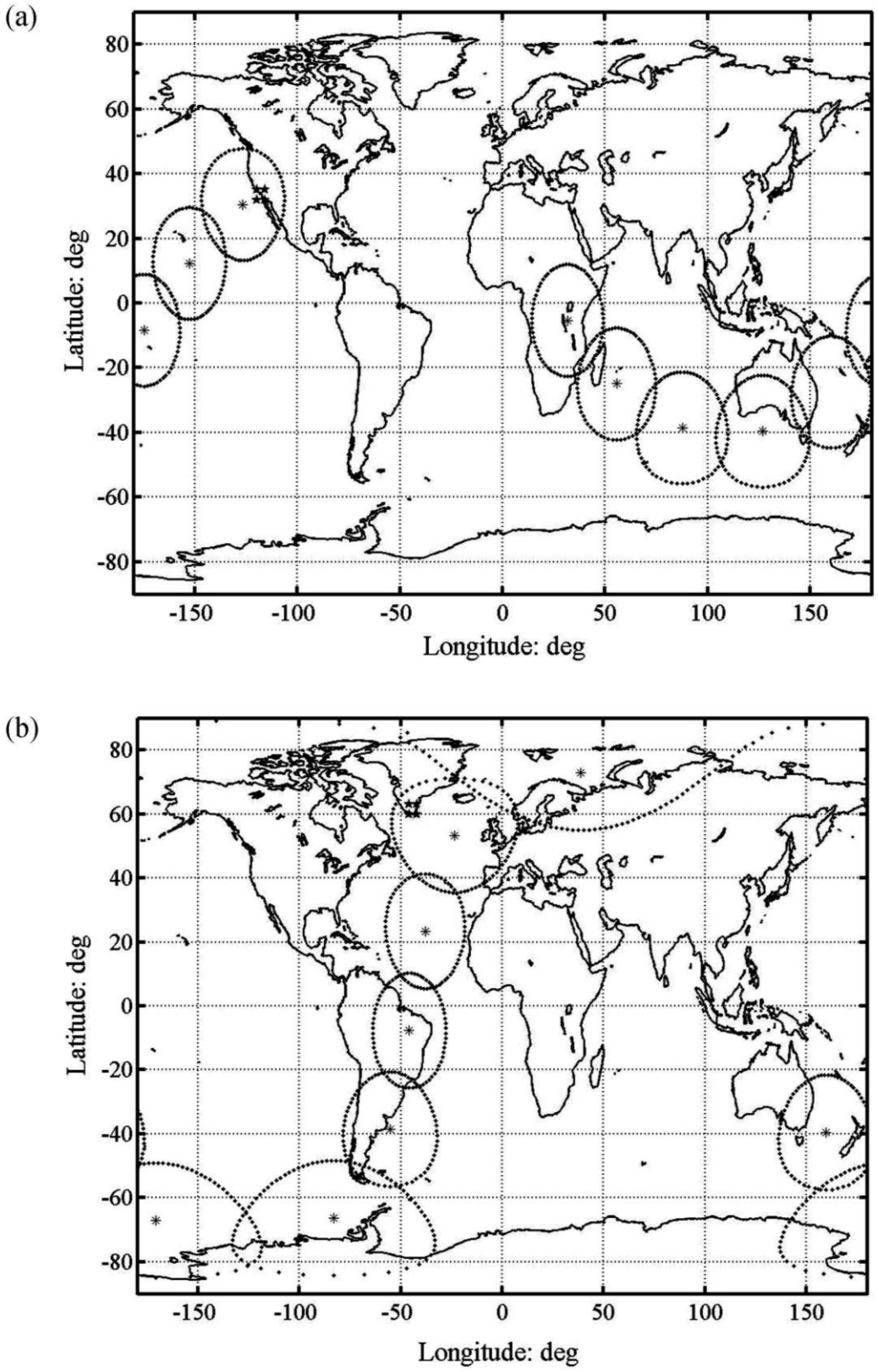

Fig. 8: Visibility spots of two 8-satellite telecommunication constellations (with $N_t = 15$ and $m = 1$) designed to fulfill requirement A, with reference to region 1 (a) and to region 2 (b)

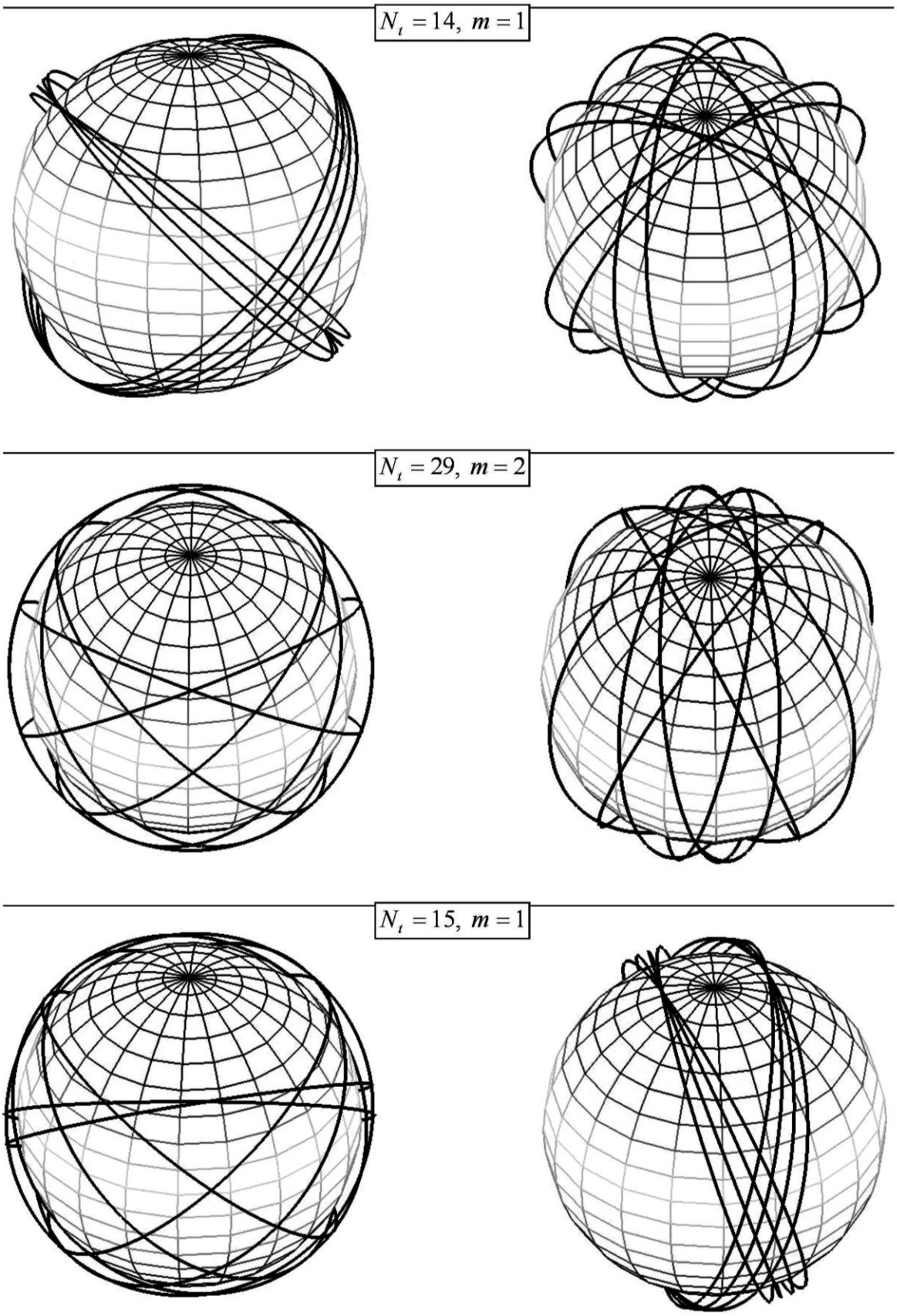

Fig. 9: Some 8-satellite telecommunication constellations optimal with respect to requirement B, with reference to region 1 (left column) and to region 2 (right column)

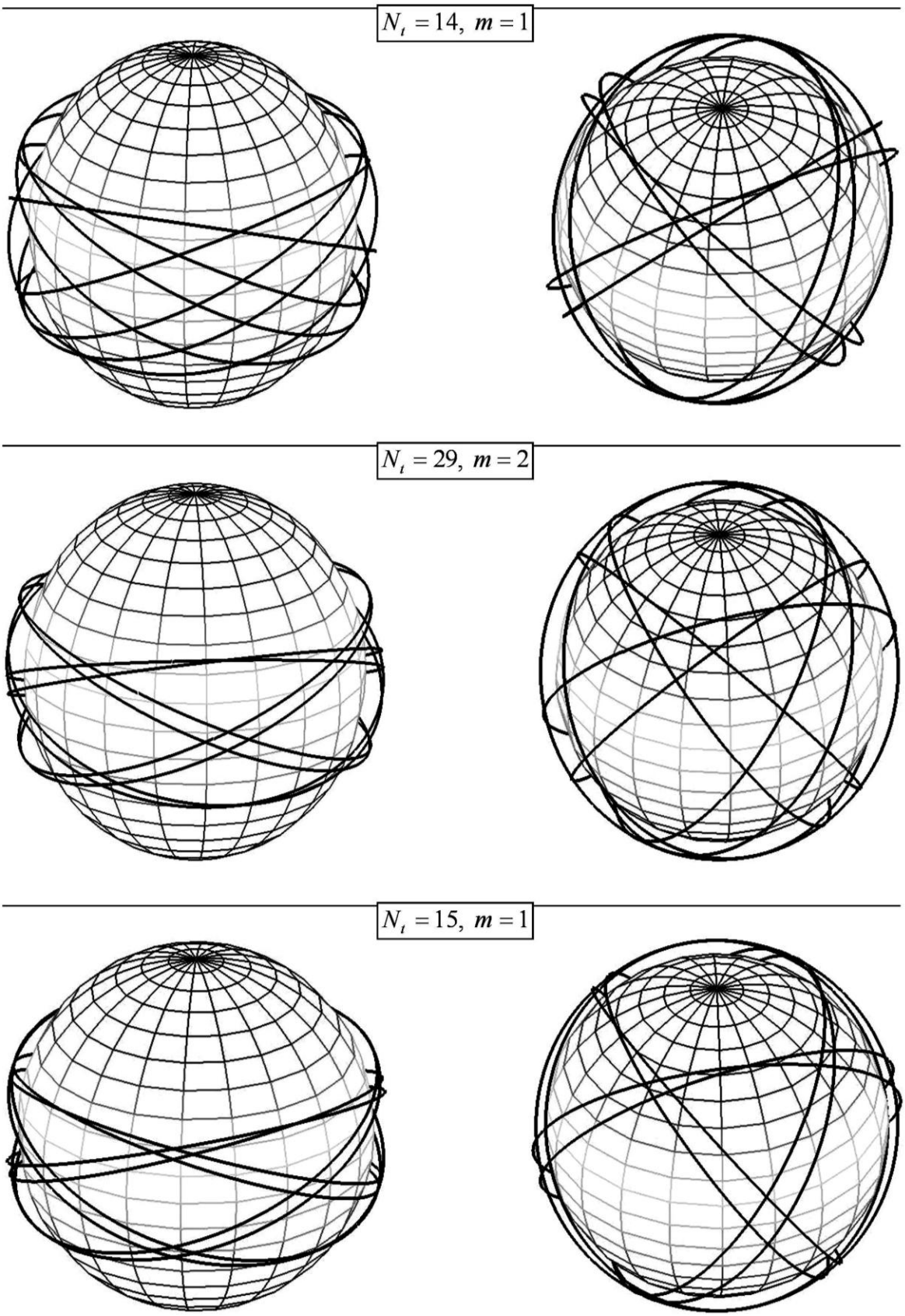

Fig. 10: Some 8-satellite monitoring constellations optimal with respect to requirement B, with reference to region 1 (left column) and to region 2 (right column)

Table 2. Constellation performance for target regions 1 and 2

Telecommunication constellation		Region 1		Region 2	
$N_t = 14,\ m = 1$		Req. A	Req. B	Req. A	Req. B
Constellation of 4 satellites	MCov (min)	49.13	15.19	49.05	22.58
	MGap (min)	733.03	45.99	552.72	44.15
Constellation of 8 satellites	MCov (min)	98.26	12.28	98.10	24.42
	MGap (min)	683.90	19.20	503.67	16.55
$N_t = 43,\ m = 3$		Req. A	Req. B	Req. A	Req. B
Constellation of 4 satellites	MCov (min)	44.03	19.12	44.96	21.92
	MGap (min)	819.64	86.83	640.47	43.50
Constellation of 8 satellites	MCov (min)	88.06	14.32	89.92	21.54
	MGap (min)	775.61	32.19	595.51	17.35
$N_t = 29,\ m = 2$		Req. A	Req. B	Req. A	Req. B
Constellation of 4 satellites	MCov (min)	41.01	18.18	42.42	10.61
	MGap (min)	812.10	86.72	636.03	43.37
Constellation of 8 satellites	MCov (min)	82.02	10.25	84.85	10.61
	MGap (min)	771.09	32.06	593.60	17.71
$N_t = 44,\ m = 3$		Req. A	Req. B	Req. A	Req. B
Constellation of 4 satellites	MCov (min)	38.56	16.05	39.95	9.99
	MGap (min)	902.24	87.40	725.74	43.33
Constellation of 8 satellites	MCov (min)	77.12	19.28	79.90	9.99
	MGap (min)	863.68	32.00	685.80	17.99
$N_t = 15,\ m = 1$		Req. A	Req. B	Req. A	Req. B
Constellation of 4 satellites	MCov (min)	33.30	14.11	34.43	10.52
	MGap (min)	885.19	91.40	714.98	43.13
Constellation of 8 satellites	MCov (min)	66.60	13.16	68.85	10.52
	MGap (min)	851.90	35.67	680.55	19.08

Table 3. Constellation performance for target regions 3 and 4

Monitoring constellation		Region 3		Region 4	
$N_t = 14,\ m = 1$		Req. A	Req. B	Req. A	Req. B
Constellation of 4 satellites	MCov (min)	13.96	6.98	14.16	6.65
	MGap (min)	967.70	105.16	1089.55	136.39
Constellation of 8 satellites	MCov (min)	27.92	4.69	28.32	6.65
	MGap (min)	953.75	50.71	1075.39	49.77
$N_t = 43,\ m = 3$		Req. A	Req. B	Req. A	Req. B
Constellation of 4 satellites	MCov (min)	12.19	5.72	12.96	4.01
	MGap (min)	1048.90	102.87	1166.33	100.79
Constellation of 8 satellites	MCov (min)	24.39	3.05	25.91	4.01
	MGap (min)	1036.70	50.34	1153.37	49.20
$N_t = 29,\ m = 2$		Req. A	Req. B	Req. A	Req. B
Constellation of 4 satellites	MCov (min)	10.94	4.51	11.81	4.12
	MGap (min)	1139.43	101.65	1153.06	118.48
Constellation of 8 satellites	MCov (min)	21.89	4.51	23.63	4.12
	MGap (min)	1128.49	49.66	1141.24	58.30
$N_t = 44,\ m = 3$		Req. A	Req. B	Req. A	Req. B
Constellation of 4 satellites	MCov (min)	9.98	2.49	10.73	2.68
	MGap (min)	1126.03	100.52	1140.53	108.51
Constellation of 8 satellites	MCov (min)	19.96	3.21	21.47	2.81
	MGap (min)	1116.05	49.35	1129.80	48.70
$N_t = 15,\ m = 1$		Req. A	Req. B	Req. A	Req. B
Constellation of 4 satellites	MCov (min)	6.59	3.30	6.81	3.41
	MGap (min)	1101.21	200.28	1116.57	230.24
Constellation of 8 satellites	MCov (min)	13.18	3.30	13.62	3.41
	MGap (min)	1094.62	48.53	1109.76	47.91

Due to the above mentioned properties of repeating orbits, the visibility intervals related to a specific region are repeated in longitude. For instance, the optimal constellations related to region 1 preserve their performance over the regions illustrated in Figures 11(a) and 11(b), which refers to the cases $(N_t + m)$ even and $(N_t + m)$ odd, respectively.

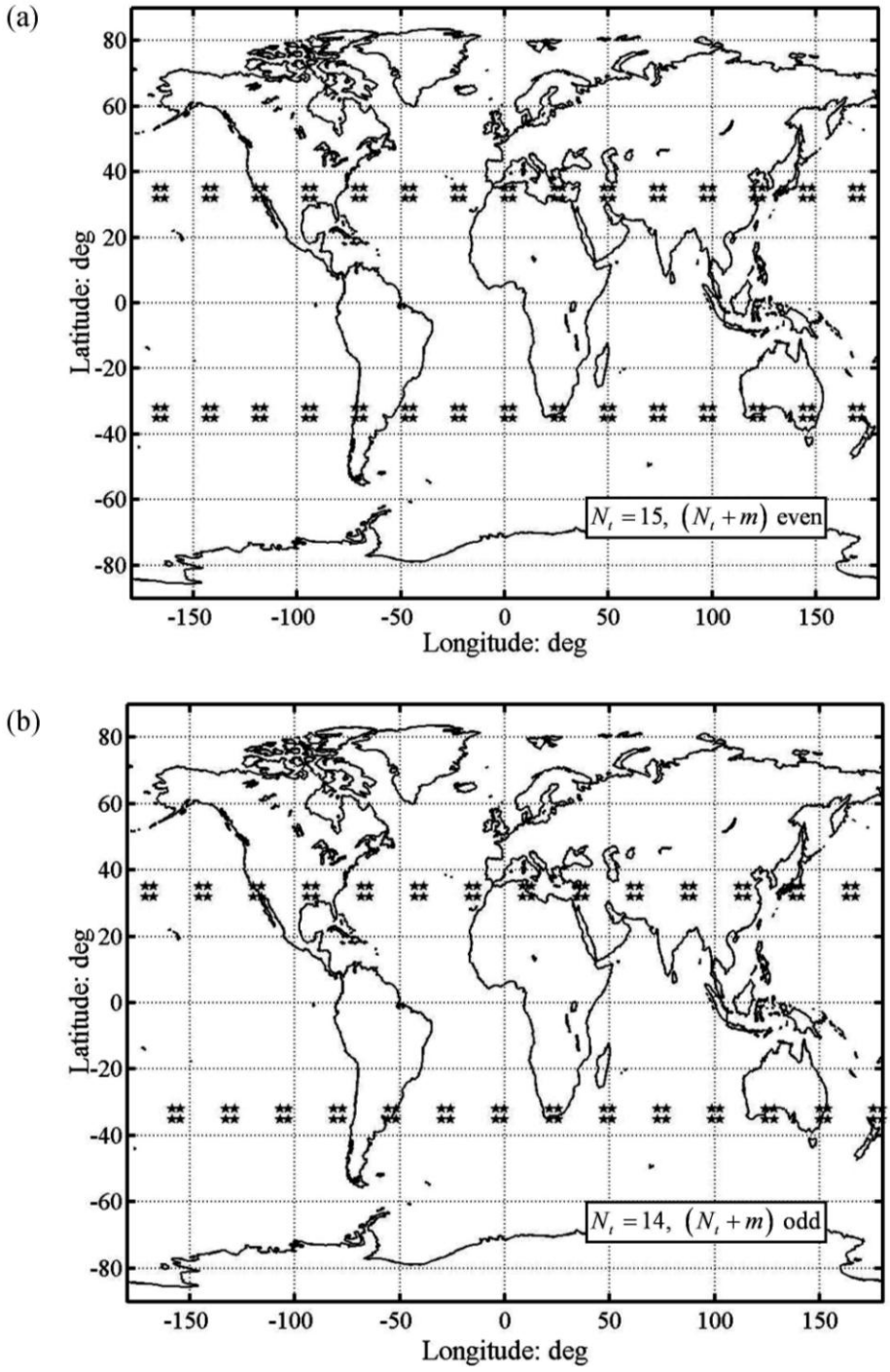

Fig. 11. Geographical regions where repeating constellations preserve their performance

6. Conclusions

This paper describes an alternative method for designing LEO satellite constellations tailored to local observation. Symmetry-based assumptions used in early works on constellations are removed, since at first glance these assumptions appear restrictive for local purposes. All the satellites are supposed to be placed in circular, equally inclined orbits at the same altitude, in order to avoid differential actions by the J_2 perturbation on each of them. Repeating orbits are employed. As shown by Hanson et al. [13] these orbits are more effective; in addition, they allow predicting the constellation performance over the period of repetition.

In this work, constellation design is based on some steps: first of all, the total duration of visibility is maximized for the first satellite that forms the constellation. Then, the motion of the remaining satellites is assumed to preserve the same visibility characteristics of the first, i.e. it is simply shifted in time. The determination of the optimal set of time delays between visible passes of distinct satellites allows identifying the optimal constellation configuration, with reference to two operational requirements, i.e. the maximization of the maximum duration coverage, or the minimization of the maximum revisit time. The visibility function, introduced in Section 4, constitutes a convenient way of representing the cascade of time intervals of visibility and gaps of non-visibility, and is used to define the correlation function, which measures the overlapping between visible passes of distinct satellites. A global search over the zeros of the correlation function allows determining the optimal constellation with reference to each of the two requirements. Some results of possible practical interest are reported in Section 5.

The method described in this research was successfully applied by the authors to LEO constellation design [14] also with reference to hybrid requirements, associated to the situations when either the maximum revisit time or the maximum coverage duration is constrained. In addition, the correlation function was employed in [15] also for eccentric orbit constellation design. In that context, the minimization of the correlation function – and not the annihilation – was pursued, and constellations ensuring the continuous coverage of a target area were found, by minimizing the overlapping between visible passes.

In conclusion, the correlation-based approach proposed in this paper seems quite efficient because computational effort is limited. This is mainly due to the analytical form of the correlation function, which, moreover, allows finding solutions with great accuracy.

Appendix 1. Physical constants

The following physical constants are used in this paper:

- Earth radius, $R_E = 6378.165$ km
- Earth planetary constant, $\mu_E = 398604.3$ km^3/sec^2
- Earth rotation rate, $\omega_E = 7.292115 \cdot 10^{-5}$ sec^{-1}
- Earth oblateness coefficient, $J_2 = 1.082627 \cdot 10^{-3}$

Appendix 2. Equatorial property of repeating ground tracks

Ground tracks of repeating satellites have a typical reticular aspect, portrayed in Figures 1 and 2. Grid α and grid β differ with regard to ascending and descending equatorial crossings, since they coincide in the former case, not in the latter. What will be demonstrated is that this feature depends on the sum $(N_t + m)$.

To do this, let $\Delta T = \pi/\dot{\theta}$ be the time interval between ascending and descending crossings. Their angular separation $\Delta\Theta$ is given by:

$$\Delta\Theta = \pi + \dot{\Omega}\Delta T - \omega_E \Delta T = \pi + \left(\dot{\Omega} - \omega_E\right)\frac{\pi}{\dot{\theta}} \tag{36}$$

For repeating satellites that complete N_t orbits in *m* nodal days the relationship (6) holds; hence, (36) becomes:

$$\Delta\Theta = \pi\left(1 + \frac{m}{N_t}\right) \tag{37}$$

Grid α corresponds to $\Delta\Theta = \vartheta \cdot 2\pi/N_t$ $(\vartheta$ integer$)$, grid β to $\Delta\Theta = \vartheta \cdot 2\pi/N_t + \pi/N_t$ $(\vartheta$ integer$)$:

Grid α: $\quad \Delta\Theta = \pi\left(1 + \frac{m}{N_t}\right) = \vartheta\frac{2\pi}{N_t}$ $\quad$ so $\quad (N_t + m) = 2\vartheta$ $(\vartheta$ integer$)$ (38)

Grid β: $\quad \Delta\Theta = \pi\left(1 + \frac{m}{N_t}\right) = \vartheta\frac{2\pi}{N_t} + \frac{\pi}{N_t}$ $\quad$ so $\quad (N_t + m) = 2\vartheta + 1$ $(\vartheta$ integer$)$ (39)

(38) and (39) state that grid α corresponds to $(N_t + m)$ even, grid β to $(N_t + m)$ odd.

References

1. Walker, J. G., “Circular Orbit Patterns Providing Continuous Whole Earth Coverage”, Royal Aircraft Establishment, Tech. Rep. 70211, Farnborough (UK), November 1970
2. Walker, J. G., “Some Circular Orbit Patterns Providing Continuous Whole Earth Coverage”, Journal of the British Interplanetary Society, Vol. 24, 1971, pp. 369-384
3. Walker, J. G., “Continuous Whole Earth Coverage by Circular Orbit Satellite Patterns”, Royal Aircraft Establishment, Tech. Rep. 77044, Farnborough (UK), March 1977
4. Ballard, A. H., “Rosette Constellations of Earth Satellites”, IEEE Transactions on Aerospace and Electronic Systems, Vol. 16, No. 5, September 1980, pp. 656-673
5. Ullock, M. H., Schoen, A. H., “Optimum Polar Satellite Networks for Continuous Earth Coverage”, AIAA Journal, Vol. 1, No. 1, January 1963, pp. 69-72
6. Rider, L., “Optimized Polar Orbit Constellations for Redundant Earth Coverage”, The Journal of the Astronautical Sciences, Vol. 33, No. 2, April-June 1985, pp. 147-161
7. Palmerini, G. B., Graziani, F., “Polar Elliptic Orbit for Global Coverage Constellations”, AAS/AIAA Astrodynamics Conference, Scottsdale, AZ, AIAA Paper 94-3720, August 1994, pp.120-129
8. Draim, J. E., “Three- and Four-Satellite Continuous-Coverage Constellations”, Journal of Guidance, Control, and Dynamics, Vol. 8, No. 6, November-December 1985, pp. 725-730
9. Ma, Der-Ming, Hsu, Wen-Chiang, “Exact Design of Partial Coverage Satellite Constellations over Oblate Earth”, AAS/AIAA Astrodynamics Conference, Scottsdale, AZ, AIAA Paper 94-3721, August 1994, pp.130-139
10. Lang, T. J., Hanson, J. M., “Orbital Constellations Which Minimize Revisit Time”, Paper AAS 83-402, Advances in the Astronautical Sciences, Vol. 54, Part 2, 1984, pp. 1071-1086
11. Lang, T. J., Williams, E. A., Crossley, W. A.,“Average and Maximum Revisit Time Trade Studies for Satellite Constellations Using a Multiobjective Genetic Algorithm”, The Journal of the Astronautical Sciences, Vol. 49, No. 3, July-September 2001, pp. 385-400
12. Lang, T. J., “A Parametric Examination of Satellite Constellations To Minimize Revisit Time for Low Earth Orbits Using a Genetic Algorithm”, Paper AAS 01-345, Advances in the Astronautical Sciences, Vol. 109, Part I, 2001, pp. 625-640
13. Hanson, J. M., Evans, M. J., Turner, R. E., “Designing Good Partial Coverage Satellite Constellations”, The Journal of the Astronautical Sciences, Vol. 40, No. 2, April-June 1992, pp. 215-239.

14. Pontani, M., Teofilatto, P., “Satellite Constellations for Continuous and Early Warning Observation: a Correlation-Based Approach”, Journal of Guidance, Control, and Dynamics, Vol. 30, No. 4, July-August 2007, pp. 910-920
15. Pontani, M., “Constellation of Repeating Satellites for Local Telecommunication and Monitoring Services”, Series on Advances in Mathematical and Applied Sciences, Vol. 75, World Scientific, 2007, pp. 513-524

Authors

M. Pontani, Scuola di Ingegneria Aerospaziale, University of Rome “La Sapienza”
via Eudossiana 16, 00184 Rome, Italy
Contacts: mauro.pontani@uniroma1.it

P. Teofilatto, Scuola di Ingegneria Aerospaziale, University of Rome “La Sapienza”
via Eudossiana 16, 00184 Rome, Italy
Contacts: paolo.teofilatto@uniroma1.it.